Structural Analysis of Historic Construction – D'Ayala & Fodde (eds)
© 2008 Taylor & Francis Group, London, ISBN 978-0-415-46872-5

Experimental shear behavior of stone masonry joints

G. Vasconcelos, P.B. Lourenço & D. Oliveira
Isise, Department of Civil Engineering, University of Minho, Guimarães, Portugal

ABSTRACT: The mechanical characterization of the shear strength properties takes a major role on the evaluation of the lateral strength of masonry shear walls by means of simplified methods or when numerical analysis based on micromodelling approach is to be followed. Thus, the present paper presents an overview of the results obtained from direct shear tests of different types of masonry joints: dry and mortar masonry joints. Besides the shear strength parameters, a good insight was achieved in the evaluation of the complete shear stress-shear load displacement diagrams.

1 INTRODUCTION

As reported in literature (Hamid & Drysdale 1980, Samarasinghe & Hendry 1980), the orientation of the mortar joints to the applied stresses takes a major role in the ultimate strength and failure modes of masonry under in-plane stress state. The influence of mortar joints acting as a plan of weakness on the composite behavior of masonry is even more relevant in case of strong unit-weak mortar joint combinations, which are characteristic of ancient stone masonry. Two basic failure modes can occur at the level of the unit-mortar interface: tensile failure (mode I) associated to stresses acting normal to joints and leading to the separation of the interface, and shear failure (mode II) corresponding to a sliding mechanism of the units or shear failure of the mortar joint.

Although several experimental studies have been carried out in the characterization of the bond shear strength of unit-mortar interfaces (Atkinson Amadio & Rajgelj 1991, Binda et al. 1997), lesser research is available on the shear behavior of dry stacked masonry joints, even if recent studies have been carried out on the behavior of dry masonry joints submitted to cyclic loading (Lourenço & Ramos 2004). On the other hand, the features of rock joints under shear behavior can be partly extended to dry masonry joints. The shear behavior of rock joints has been played an important role in the scope of rock mechanics research. In particular, several experimental and numerical studies pointed out the role of the surface roughness on the cyclic shear behavior of natural rock joints (Lee et al. 2001, Huang et al. 2002).

The relation between normal and shear stresses has a major role in the shear behavior of masonry joints, governing its failure mode (Hamid & Drysdale 1980). For pre-compression stresses above a certain level, the shear strength decreases and a combined shear-splitting failure or splitting of the units occur. In case of shear failure along the joint by slipping of the units along the joint, an increase of the compression normal to bed joint leads to an increase of the shear strength. As has been widely reported (Atkinson et al. 1989, Riddington & Ghazali, 1990), the shear strength of masonry under moderate normal stresses, for which the nonlinear behavior of mortar is negligible and the friction resistance takes the central role, can be given by the Coulomb criterion:

$$\tau = c + \mu\sigma \tag{1}$$

where c is the shear strength at zero vertical load stress (usually denoted by cohesion) and μ is the friction coefficient. For dry joints the cohesion is assumed to be zero. It should be kept in mind that the failure envelop given by eq.1 describes only a local failure and can not be directly related to the shear failure of masonry walls submitted to in-plane horizontal loads (Mann & Müller 1982, Atkinson et al. 1989, Calvi et al.1996).

In addition to the knowledge of the mechanical properties from masonry components, namely units and mortar, the analysis of masonry behavior under in-plane loading is only possible if information about the local composite behavior and the interaction between units and mortar is available.

Therefore, the present work deals with the mechanical characterization of the shear behavior of dry and mortar masonry joints (cohesion, friction angle and dilatancy). In order to attain such goal, an experimental program was defined, including direct shear tests conducted on dry and mortar masonry joints. Besides

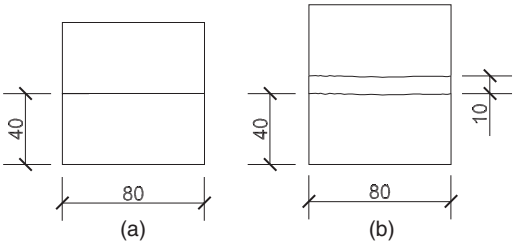

Figure 1. Masonry specimens; (a) dry joints; (b) mortar joints.

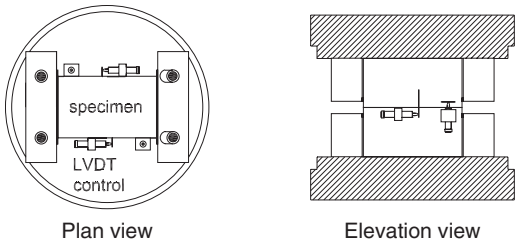

Figure 2. Arrangement of the LVDTs for measuring of the relative horizontal and vertical displacements.

ensuring mechanical properties for numerical simulations of the in-plane behavior of stone masonry wall structures, the adopted testing program provides also the fundamental information about the shear behavior of two different masonry joints.

2 EXPERIMENTAL DETAILS

2.1 *Test specimens and procedure*

Although triplet tests have been adopted as the European standard method (EN1052-3 2002) to perform shear tests in mortar joints, the shear strength properties of dry and mortar joints were obtained by means of direct shear tests conducted on couplet specimens, see Figure 1 (Vasconcelos 2005). In fact, in the triplet test, the two joints do not fail at the same time and the analysis of the experimental results is rather complex, Lourenço et al. (2004).

The shear tests were carried out in a servocontrolled universal testing machine CS7400S. This equipment is composed by two independent hydraulic actuators used to transmit normal and shear loads, able to operate under force or displacement control. The features of the testing equipment and the existing loading platens imply that the most suitable testing sample is composed by two units with geometry and dimensions indicated in Figure 1 and a single dry or mortar joint, similarly to Pluijm (1999) and Hansen et al. (1998). The surface of the dry masonry units adopted here is smooth resulting from sawing the specimens, whereas the joint surface of the units of the mortar assemblages presents enough roughness to achieve appropriate adherence conditions and thus more realistic masonry can be simulated. The detailed experimental characterization of this type of granite can be seen in Vasconcelos et al. (2007). The specimens were placed between two thick steel plates and attached to the steel platens by steel bolts, so that shear force could be transmitted. Thin steel sheets were attached to the steel plates to concentrate the shear load as close as possible in the bed joint, aiming at preventing bending moments and provide a more uniform shear stress distribution.

In addition, two thin sheets of Teflon were interlayered between the steel platens and the specimens to minimize bending effects. In order to guarantee right angle surfaces, the specimens were suitably ground using a rectifying machine. The same procedure was used in the contact surfaces between both units of the specimens to ensure the maximum contact area in case of dry joints. In fact, according to Hansen (1999), the uneven stress distribution can also be attributed to the non-uniform distribution of the material along bed joints. In both types of specimens, when necessary, a thin layer of glue was placed at the surface in contact with the steel platens in order to provide perfectly leveled surfaces. The confinement of the specimens was improved for load reversal by means of a couple of steel rods fixed to the steel plates through metallic bolts. This arrangement is particularly useful in the cyclic tests but was also used in case of monotonic tests. The numerical assessment of the effectiveness of the test setup was performed by Lourenço and Ramos (2004) based on a finite element model. It was concluded that although a deviation on the stresses occurs in the zone adjacent to the steel plates, an almost uniform normal and shear stress distribution is achieved in 63% of the extent of the bed joint.

In order to simulate the usual range of normal stresses existing in ancient masonry structures three distinct pre-compression stress levels were applied under force control, $\sigma = 0.5\,\mathrm{N/mm^2}$, $\sigma = 0.75\,\mathrm{N/mm^2}$ and $\sigma = 1.0\,\mathrm{N/mm^2}$ in dry joints under monotonic and cyclic loading. An additional pre-compression stress level corresponding to $\sigma = 1.25\,\mathrm{N/mm^2}$ was considered for the monotonic tests carried out on unit-mortar assemblages. Three specimens were tested for each level of pre-compression for both types of masonry joints. The possible influence of the moisture content on the shear response of dry masonry joins was investigated by considering dry and saturated conditions. Although the horizontal actuator is servo-controlled, the control was made using the horizontal LVDT adjacent to bed joint because a more stable response was found. The disposition of the LVDTs for measuring the horizontal and vertical displacements of the joint is depicted in Figure 2.

The relative horizontal displacement of the joint was measured by the horizontal LVDTs placed at each side of the specimen. Although the LVDTs were fixed to the unit through the supports that were glued to it, the influence of the shear deformation of the units should be marginal in the measured final deformation (Hansen 1999). The vertical displacements of the joint were measured by the LVDTs placed at the opposite corners of the specimen. The relative vertical displacements were monitored in case of dry joints for assessing the possible dilatant behavior of the joints. Nevertheless, technical problems did not allow to measure relative vertical displacements in mortar joints, as tests were conducted in a subsequent phase. Both shear and normal stresses were measured and recorded by the horizontal and vertical load cells of 22 kN capacity.

3 ANALYSIS OF RESULTS

3.1 *Monotonic behavior of dry joints*

The shear load-shear displacement diagrams for distinct pre-compression stress levels resulting from the monotonic tests conducted on dry and saturated specimens are displayed in Figure 3a and Figure 3b respectively. The shear displacement is the result of averaging the measurements recorded by both LVDTs placed at each side of the specimen. The shear stress is calculated by the following expression:

$$\tau = \frac{H}{A} \tag{2}$$

where H is the load in the horizontal actuator and A is the cross area of the joint section. The normal stress is also calculated from the normal pre-compression load, N, and is also based on the total area of the cross section as:

$$\sigma = \frac{N}{A} \tag{3}$$

From the responses in Figure 3, no significant differences were detected between dry and saturated specimens and the peak shear strength was found to increase as the normal stresses increase. By comparing the peak shear stresses, lower values were obtained in case of saturated specimens and higher scatter was found when the maximum pre-compression level ($\sigma_0 = 1.0\,\mathrm{N/mm^2}$) was applied.

Four stages can be identified in the shear stress-shear displacement diagrams. The pre-peak behavior is characterized by a linear extent for low levels of shear stress, associated to the contact of the joint interface, and by a clear non-linear stretch until peak shear is reached. These features can be confirmed from Figure 3, where the pre-peak part is highlighted. A

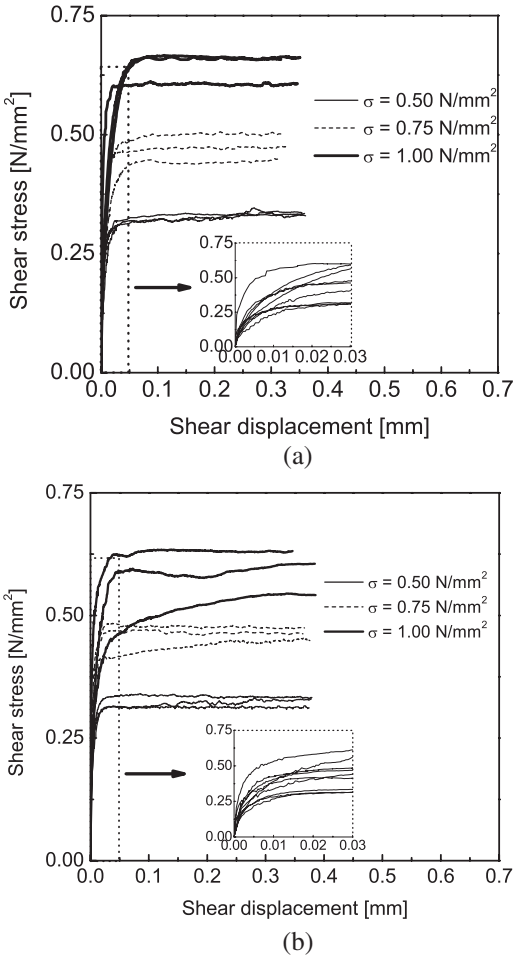

Figure 3. Shear stress-shear displacement diagrams in dry joints; (a) dry specimens; (b) saturated specimens.

plateau is found at peak stress, as the shear behavior of dry masonry joints under monotonic loading exhibits considerable plastic deformations associated to the inelastic sliding.

Similarly to what has been reported in literature (Misra 2002, Huang et al. 2002) no shear softening was recorded after peak stress for smooth surfaces, unlike rough rock joints that exhibit remarkable lowering of the shear resistance as the plastic shear displacement increases due to the roughness fracture.

3.2 *Monotonic behavior of mortar joints*

The shear stress-shear displacement diagrams of mortar joints with respect to all levels of pre-compression are shown in Figure 4a. The horizontal displacement is considered as the average of the displacements

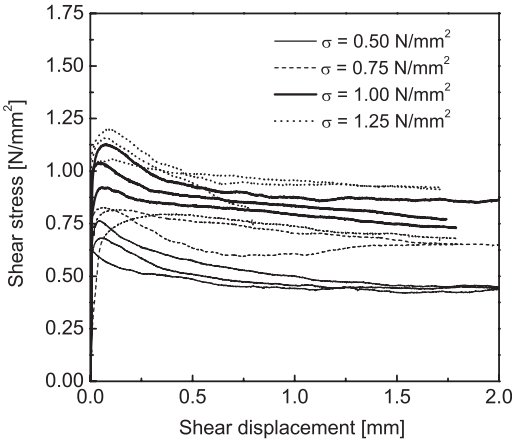

(a)

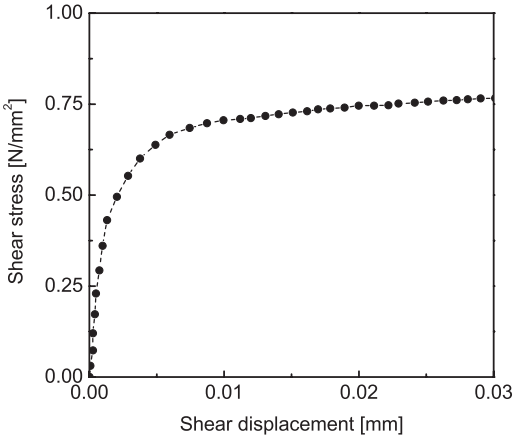

(b)

Figure 4. Shear behavior of mortar joints; (a) shear stress-shear displacement diagram; (b) pre-peak nonlinearity.

recorded by the two horizontal LVDTs located at each side of the specimen and the shear stress is calculated according to eq. 2. The general shape of the shear stress-shear displacement is characterized by a sharp initial linear stretch. The peak load is rapidly attained for very small shear displacements. Similarly to what was reported for dry masonry joints, nonlinear deformations develop in the pre-peak regime, see Figure 4b.

After peak load is attained there is a softening branch corresponding to progressive reduction of the cohesion, until reaching a constant dry-friction value. This stabilization is followed by the development of large plastic deformations.

As required, the shear tests were carried out without significant fluctuations of vertical load (less than

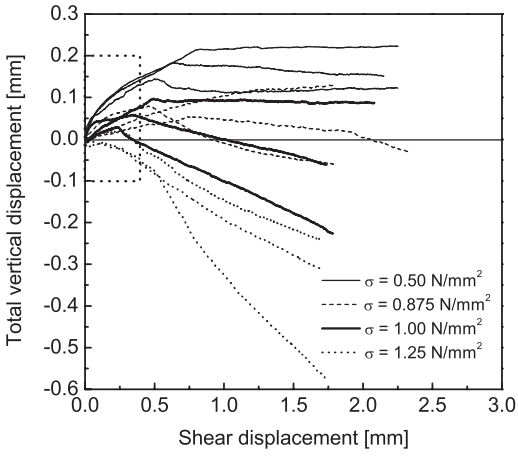

Figure 5. Relation between total vertical displacement and shear displacement.

2%). Note that the shear tests are conducted under horizontal displacement control. This further assesses the validation of the test setup.

In spite of the fact that the relative local vertical displacements of the joint could not be measured due to technical problems with the LVDTs, the total vertical displacement was recorded by the internal LVDT located inside the vertical actuator. The evolution of this displacement with the shear displacement is displayed in Figure 5, where in the greater number of the tests two distinct phases can usually be distinguished. Firstly, the uplift of the joint is expressed by increasing positive vertical displacements, which is particularly remarkable for low normal stresses. The nonlinear evolution of the displacements provides variable dilatancy assuming decreasing values as the shear displacement increases. This behavior is connected to the changes on the interfaces due to surface wearing. It is observed that the shear displacement associated to the maximum value of the vertical displacement is close to the horizontal displacement corresponding to the stabilization of the shear stress.

The dilatant behavior reflects, to great extent, the distinct shear failure modes obtained in the specimens submitted to different normal stresses. In fact, for low levels of pre-compression, shear failure occurs at the unit-mortar interface along one unit face or, more frequently, divided between two unit faces, see Figue 6. For the larger normal stress level ($\sigma = 1.25\ \mathrm{N/mm^2}$), the failure is only localized in the mortar and a larger amount of small mortar particles were found to be detached. No damage was visible in the stone units in all cases.

During the regime of pure friction the vertical displacement remains constant or progressively

Figure 6. Typical Failure mode for the lower compression level ($\sigma = 0.5\,\mathrm{N/mm^2}$).

decreases, which is more significant as the level of pre-compression increases, exhibiting even negative values in some specimens submitted to pre-compression levels of $\sigma = 0.75\,\mathrm{N/mm^2}$ and $\sigma = 1.00\,\mathrm{N/mm^2}$. This seems to indicate that as the pure shear develops, the wearing of the surface joints leads to compaction in the case of the porous lime mortar used. For the larger pre-compression level ($\sigma = 1.25\,\mathrm{N/mm^2}$), only compaction of the specimen was recorded, which is revealed by the negative values of the total vertical displacements, resulting from the higher level of degradation of the mortar joint associated to the continuous friction.

3.2.1 *Cyclic behavior of dry joints*

The typical shear stress-shear displacement diagrams obtained in direct cyclic shear tests conducted in masonry joints of dry and saturated specimens are displayed in Figure 7 for the level of pre-compression $\sigma = 0.75\,\mathrm{N/mm^2}$.

The shear behavior of dry joints during the first cycle agrees with the monotonic diagrams exhibiting nonlinearity in the pre-peak regime and post-peak plastic deformations. Apart from the distinct values of the peak shear stress, no significant differences in the shape of the diagrams can be found in the range of the tested normal stresses, which is valid for both dry and saturated specimens.

Figure 8 shows the shear stress-shear displacement diagrams for the first and last cycles of loading corresponding to distinct levels of pre-compression. Although minor differences are found in the shear strength during the reversal cycles among the distinct pre-compression levels, there seems to be a more systematic tendency for a slight increase between the first and the last cycles as the vertical pre-compression takes higher values. This effect is more clear in dry specimens. Note that from the monotonic shear stress-shear displacement diagrams, it is observed that for a shear displacement of 0.1 mm, the maximum shear forces were already reached.

This result is also in agreement with the findings reported by Lee et al. (2001) concerning direct shear tests conducted on smooth joints of granite, which referred that the preferential degradation of quartz

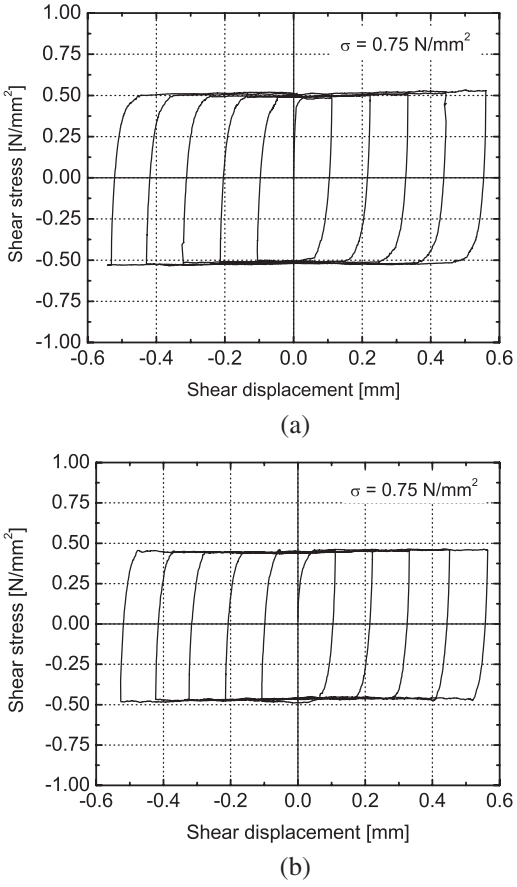

Figure 7. Shear stress-shear displacement diagrams under cyclic loading for $\sigma = 0.75\,\mathrm{N/mm^2}$; (a) dry specimens; (b) saturated specimens.

grains against other rock-forming minerals could provide the stick-slip on the surface of granite. When an analysis of the normal displacement-shear displacement diagrams is carried out, it is possible to observe a more visible tendency for compaction associated to the wearing of the joint surface.

From the normal-shear displacement diagrams, it is possible to conclude that the values of dilation/compaction are not greater than ± 0.06 mm, which shows good agreement with the values reported by Lourenço & Ramos (2004) for dilation obtained on sandstone smooth dry joints and with the results pointed out by Homand et al. (2001) for hammered granitic joints. In both cases, the degradation mechanism is dominant over the phenomenon of dilatancy. Therefore, it is reasonable to assume that this type of smooth rock joints is non-dilatant. This result is also enlarged to the shear behavior of saturated specimens. In fact, it is well known that the dilatant behavior

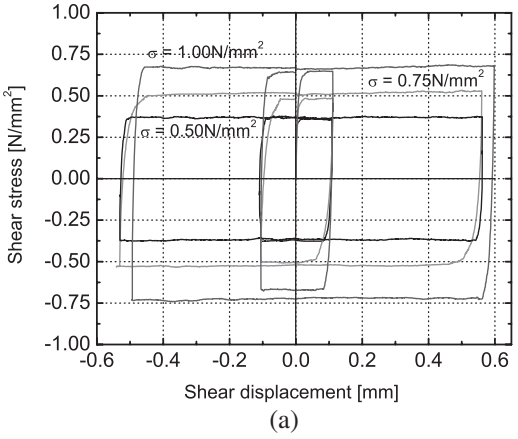

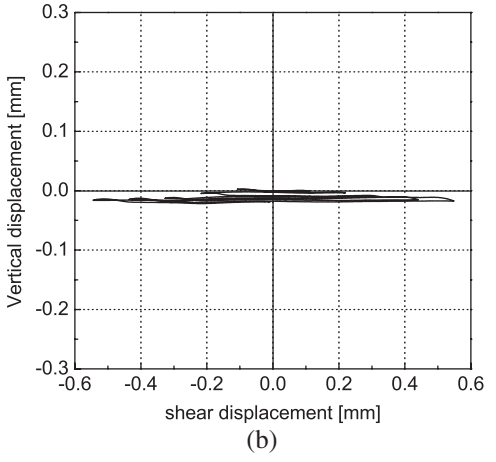

Figure 8. Characteristic aspects of the shear behavior of dry joints; (a) evolution of the shear stress-shear displacement diagrams between the first and the last cycle of reversal loading; (b) compaction due to the wearing of the joint surface.

of rock joints is highly dependent on both roughness of the joint surface and the level of vertical pre-compression (Amadei et al. 1998; Huang et al. 2002, Misra 2002). As referred by these authors, in rough joints lower dilation is obtained at high normal stresses and for increasing shear displacements dilatancy tends to exhibit decreasing values.

Based on the shear stress-shear displacement diagrams, it is observed that the shear behavior of dry joints is characterized by an approximately constant stiffness followed by marked nonlinearity close to the peak load in the loading branches. On the other hand, the stiffness of the unloading branches exhibits always considerable high values when compared with the stiffness obtained in the loading and reloading cycles. The corrected displacement of the dry joint can be

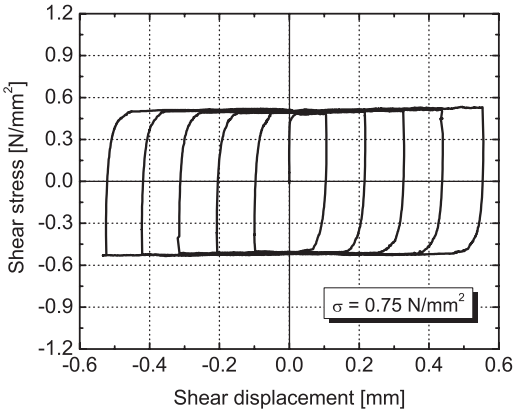

Figure 9. Correction of the measured shear displacement-dry specimens.

obtained by removing the elastic deformation of the unit reading:

$$u_{joint} = u_{meas} - \frac{\tau}{k_u} \quad (4)$$

where u_{meas} is the shear displacement given by the horizontal LVDTs, τ is the shear stress for a given displacement and k_u is the stiffness calculated in the unloading branches. It is possible to confirm that the elastic deformation of the units has a minor role in the total shear displacement of dry joint, see Figure 9.

The shear behavior of dry joints is thus characterized by significant non-linear deformations in the pre-peak stage and perfect plastic deformations after peak stress resulting from the characteristic sliding failure mode. The former characteristic of the shear behavior of dry joints was already pointed out by Lourenço & Ramos (2004). Apart from the nonlinearity in the pre-peak regime, the envelop of the diagrams is also in good agreement with the shape of the shear stress-shear displacement diagrams indicated by Lee et al. (2001), also for smooth sawn-cut granitic joints.

3.3 *Shear strength-normal stress diagrams*

Figure 10 shows the relationships between the values of the shear strength obtained in the monotonic tests and in the first cycle of the cyclic tests for dry and saturated conditions as a function of the normal stress. For both specimens, an expressive linear correlation was attained between normal and shear stress, which confirms the initial assumption that the shear strength is well described by Coulomb's friction law.

The slight decrease on the shear strength obtained on saturated specimens is here reflected by the lower value of the friction coefficient, being 0.65 and 0.60 the values that were achieved for dry and saturated

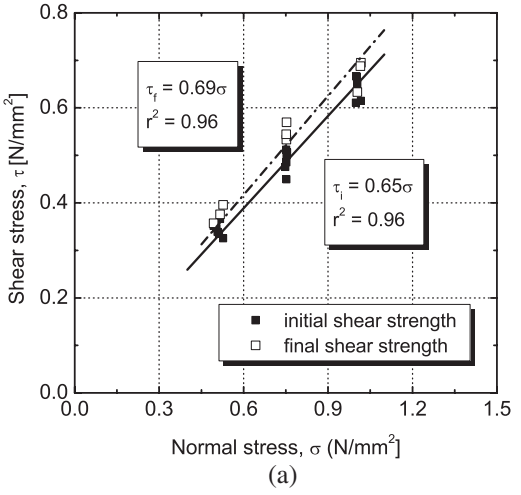

(a)

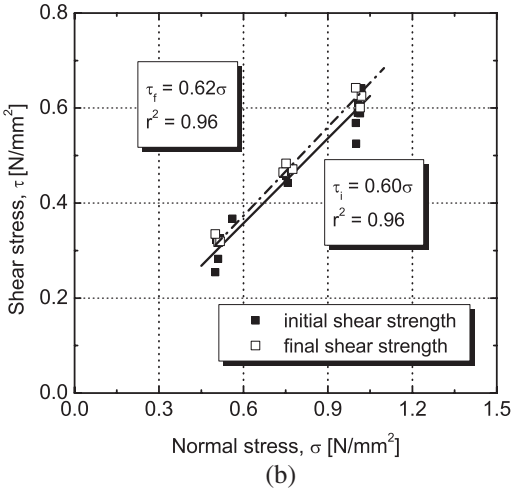

(b)

Figure 10. Characteristic aspects of the shear behavior of dry joints; (a) evolution of the shear stress-shear displacement diagrams between the first and the last cycle of reversal loading; (b) compaction due to the wearing of the joint surface.

specimens, respectively, corresponding to a lowering of the friction coefficient of approximately 10%. The influence of the moisture content on the shear strength of rock joints was also investigated by Geertsema (2002) that pointed out a decrease on the friction coefficient on saturated specimens ranging between 10° and 22.4° for mudstone. The results are obviously not comparable because the materials are considerable different.

The friction angle corresponding to dry joints is slightly larger than the value pointed out by Lourenço & Ramos (2004) for specimens composed by sandstone sawn units tested under dry conditions ($\mu = 0.63$) and somewhat lower than the value

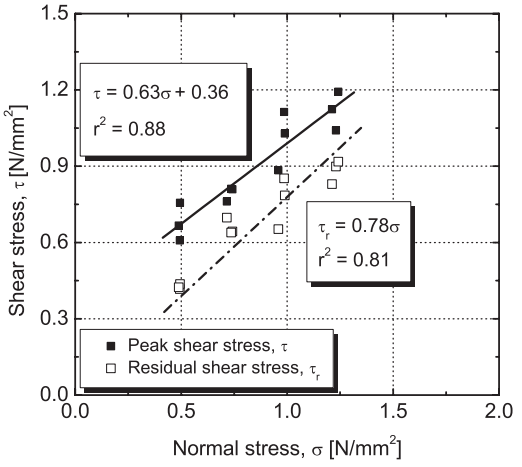

Figure 11. Relation between peak and residual shear stresses with normal stress.

indicated by Lee et al. (2001) for sawn-cut granitic joints ($\mu = 0.69$). The narrow range of values for the friction angle seems to indicate that no significant differences for this property should be expected among distinct types of natural stone under similar roughness surface conditions. For the range of vertical stresses considered, the shear strength should be more sensitive to the roughness characteristics of the bed joint surface than to the material properties or even mineralogical composition.

By comparing the values of the initial and final frictional resistance, it can be seen that there is a small increase of the frictional resistance in the last cycle, being the difference more expressive in case of dry specimens. This result confirms the tendency for the slight slipping of the shear stress-shear displacement diagrams previously referred, which can be the result of the wearing of the granitic surface. It is believed that this effect is highlighted due to the considerable porosity of this type of granite.

It should be stressed that in spite of the use of sawn-cut units to characterize the mechanical shear behavior of dry joints of masonry walls discussed later, the experimental investigation on the shear behavior of random rough dry joints, including the definition of the characteristic diagrams, failure criteria and dilatant behavior, would characterize more realistically the mortarless masonry joints existing in ancient masonry construction.

The relation between the peak and residual shear stress with the normal stress is displayed in Figure 11. Significant correlation coefficients were obtained by fitting linear functions to the experimental data composed by peak and residual shear strength, with coefficients of correlation of $r^2 = 0.88$, and $r^2 = 0.80$,

respectively. This means that for the range of pre-compression levels tested, the peak and residual shear strength of the bed joint can be reasonably described by means of the Coulomb's friction law given by eq. 1. Therefore, the linear approach provides shear strength characteristics of the mortar joint, cohesion, c, and friction coefficient, μ. A value of cohesion about 0.36 N/mm^2 and the tangent of the friction angle, $tan\phi$, equal to 0.63, corresponding to a friction angle of 32.2°, were attained for the peak strength. The residual shear strength can be calculated with reasonable accuracy from a friction coefficient of 0.78. This value can be used for evaluation of the shear sliding resistance of walls or piers submitted to seismic action failing along horizontal sliding joints. The strength values, particularly the bond strength, are greatly dependent on the moisture content and porosity of the units and on the strength and composition of mortar as well as on the nature of the interface (Amadio & Rajgelj 1990). Binda et al. (1994) pointed out that when strong mortar is considered, the strength of the units can also regulate the shear behavior of the joints. This yields that a wide range of shear strength values have been pointed out for various combinations of units and mortar.

Mann & Muller (1982) indicated a mean friction coefficient of approximately 0.65 on brick-mortar assemblages and a cohesion ranging from 0.15 up to 0.25, depending on the mortar grade. From the results of direct shear tests carried out by Pluijm (1999), the coefficient of internal friction ranges between 0.61 and 1.17, whereas cohesion varies from 0.28 up to 4.76, depending on different types of units and mortar. Table 1 summarizes other results published in literature referring to the shear strength properties for different combinations of materials.

Table 1. Shear strength properties for different unit-mortar assemblages.

Source	units	mortar	c (MPa)	μ
Atkinson (1989)	Old clay	1:2:9 (13)	0.127	0.695
	Old clay	1:2:9 (7)	0.213	0.640
	New clay	1:1.5:4.5	0.811	0.745
Amadio and Rajgeli (1990)	Solid bricks	Cement Lime-cement	0.65	0.723
Magenes (1992)	Solid bricks	Hydraulic lime	0.206	0.813
		Lime mortar	0.081	0.652
Binda *et al*. (1994)	Sandstone	Hydraulic lime	0.33	0.74
	Calcareous	Hydraulic lime	0.58	0.58
Roberti *et al*. (1997)	Bricks	Hydraulic lime mortar	0.23	0.57
Lourenço *et al*. (2004)	Hollow bricks	Micro-concrete	1.39	1.03
This study	Granite	Lime mortar	0.359	0.630

4 CONCLUSIONS

The experimental characterization of masonry assemblages and masonry components used in the shear walls discussed in Chapter 6 is addressed, focusing on the strength properties of dry masonry joints and the unit-mortar interface, as well as on the compressive properties of the masonry.

A set of direct shear tests was conducted on couplet specimens, either considering dry or mortar joints. From these tests it was possible to derive the shear strength properties, namely cohesion and friction coefficient. Besides, the complete shear stress-shear displacement diagrams enabled a better insight into the shear behavior of these assemblages. An elastic perfectly plastic diagram was found to characterize the monotonic and the cyclic envelope of shear tests conducted in dry masonry joints. No significant differences in the frictional behavior of dry joints under distinct moisture contents were found. A reduction of nearly 5% was recorded on the friction coefficient changing the moisture condition from dry to saturated. Low differences were found between the peak and residual friction angle for dry masonry joints under distinct moisture conditions. No dilatancy was found to characterize the shear behavior of dry masonry joints.

Similarly, an extended plastic branch characterizes the residual post-peak shear behavior of mortar masonry joints. After a reduction of approximately 25% of the peak strength, the shear stress stabilizes with considerable level of plastic deformations. The measured total vertical displacement revealed a tendency for the mortar joint dilation to decrease as the normal stress increases. Only for a pre-compression of 0.5 N/mm^2 a systematic expansive trend was verified up to peak stress. For this case, it was found that dilatancy decreases significantly as the shear displacement increases.

REFERENCES

Amadio, C., Rajgelj, S. 1991. Shear behavior of brick-mortar joints, Masonry International, 5 (1), 19–22.

Atkinson, R.H., Amadei, B.P., Saeb, S., Sture, S. 1989. Response of masonry bed joints in direct shear, Journal of Structural Engineering, 115 (9), 2277–2296.

Binda, L., Fontana, A., Mirabella, G. 1994. Mechanical behavior and stress distribution in multiple-leaf stone walls, 10th International Brick Block Masonry Conference, Calgary, Canada, 51–59.

Calvi, G.M., Kingsley, G.R., Magenes, G. – Testing masonry structures for seismic assessment, Earthquake Spectra, Journal of Earthquake Engineering Research Institute, 12(1), 145–162, 1996.

EN 1052-3, Methods of test for masonry: Part 3 – Determination of initial shear strength, 2002.

Geerstsema, A.J. 2002. The shear strength of planar joints in mudstone, International Journal of Rock Mechanics and Mining Sciences, 39, 1045–1049.

Hamid, A.A., Drysdale, R.G. 1980. Behavior of brick masonry under combined shear and compression loading, Proc. 2nd Canadian Masonry Conference, 314–320.

Hansen, K.F. 1999. Bending and shear tests with masonry, SBI Bulletin 123, Danish Building Research Institute, p. 36.

Hansen, K.F., Nykänen, E., Gottfredsen, F.R. 1998. Shear behavior of bed joints at different levels of precompression, Masonry International, 12 (2), 70–78.

Homand, F., Belem, T., Souley, M. 2001. Friction and degradation of rock joint surfaces under shear loads, International Journal for Numerical and Analytical Methods in Geomechanics, 25, 973–999.

Huang, T.H., Chang, C.S., Chao, C.Y. 2002. Experimental and mathematical modeling for fracture of rock joint with regular asperities, Engineering Fracture Mechanics, 69, 1977–1996.

Lee, H.S., Park, Y.J., Cho, T.F., You, K.H. 2001. Influence of asperity degradation on the mechanical behavior of rough rock joints under cyclic shear loading, International Journal of Rock Mechanics and Mining Sciences, 38, 967–980.

Lourenço, P.B., Barros, J.O., Oliveira, J.T. 2004. Shear testing of stack bonded masonry, Construction and Building Materials, 18, 125–132.

Lourenço, P.B., Ramos, L.F. 2004. Characterization of cyclic behavior of dry masonry joints, Journal of Structural Engineering, 130 (5), 779–786.

Mann, W., Müller, H. 1982. Failure shear-stressed masonry – an enlarged theory, tests and application to shear walls, Proc. British Ceramic Society, 30, 223–235.

Misra, A. 2002. Effect of the asperity damage on shear behavior of single fracture, Engineering Fracture Mechanics, 69, 1997–2014.

Pluijm, R.V.D.1999. Out-of-Plane bending of masonry, behavior and strength, PhD thesis, Eindhoven University of Technology. ISBN 90-6814-099-X.

Riddington, J.R., Ghazali, M.Z. 1990. Hypothesis for shear failure in masonry joints, Proc. Instn. Civ. Engrs, 89, 89–102.

Samarasinghe, W., Hendry, A.W. 1980. *The tensile of brickwork under biaxial tensile and compressive stress*, Proc. 7th International Symposium on Load Bearing Brickwork, London, 129–139.

Vasconcelos, G. 2005. Experimental investigations on the mechanics of stone masonry: characterization of granites and behavior of stone masonry shear walls, PhD thesis, University of Minho, Portugal.

Vasconcelos, G., Lourenço, P.B., Alves, C.A.S, Pamplona, J. 2007. Prediction of the mechanical properties of granites by ultrasonic pulse velocity and Schmidt hammer hardness, 10th North American Masonry Conference, (in press).